nature portfolio

https://doi.org/10.1038/s41586-026-10819-7

Supplementary information

Efficient and precise programmable DNA knock-in without double-strand breaks

In the format provided by the authors and unedited

Table of Contents

This file contains Supplementary Figures 1-4, Supplementary Tables 1-7, Supplementary Notes 1-5 and Supplementary References.

Supplementary Figures p.2-7

Supplementary Fig. 1: Representative gating/sorting strategy for flow cytometry and FACS analyses used in the study

Supplementary Fig. 2: The profiles of indels in uninserted alleles after Cas9-based editing

Supplementary Fig. 3: Integration of *LIPA* cDNA into the *AAVS1* locus in homozygous *LIPA*$^{894G>A}$ mutant HEK293T cells

Supplementary Fig. 4: Uncropped original gel images

Supplementary Tables p.8-18

Supplementary Table 1: sgRNA sequences used in the study

Supplementary Table 2: Plasmids used in the study

Supplementary Table 3: Main reagents used in the study

Supplementary Table 4: Primers for donor preparation

Supplementary Table 5: Primers used for HTS of on-target indels

Supplementary Table 6: PEM-seq adapters and primers

Supplementary Table 7: Primers for qPCR, translocations and genotyping

Supplementary Notes p.19-28

Supplementary Note 1: Investigating the molecular mechanisms of KNIT editing

Supplementary Note 2: Theoretical calculations on Cas9-mediated repeated editing with indel-specific sgRNAs

Supplementary Note 3: Generation and validation of homozygous *LIPA*$^{894G>A}$ HEK293T cell lines

Supplementary Note 4: Protein expression and purification

Supplementary Note 5: The sequences of KE1 and KE2

Supplementary References p.29-30

Supplementary Fig. 1 | Representative gating/sorting strategy for flow cytometry and FACS analyses used in the study

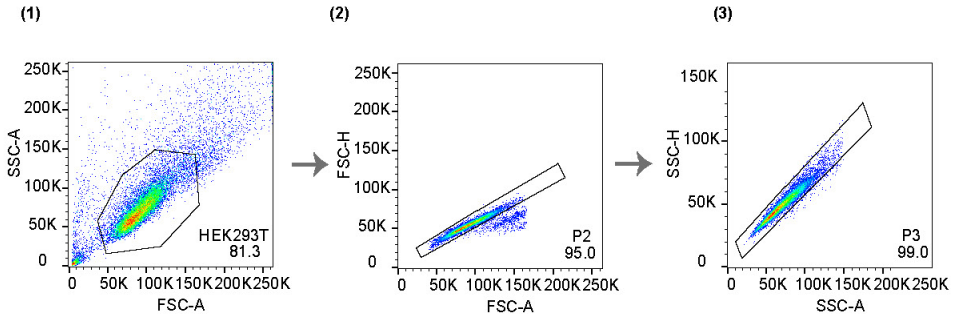

The flow cytometry and FACS analyses in this study were performed using the indicated gating/sorting strategy. Positive cell populations were subsequently determined according to the corresponding negative control groups. This strategy was applied to all flow cytometry and FACS analyses in this study.

Supplementary Fig. 2 | The profiles of indels in uninserted alleles after Cas9-based editing

a, The percentages of top on-target indels within uninserted alleles after Cas9-mediated *P2A-EGFP* (813 bp) insertion at the *H2B* locus. Related to **Fig. 2f** right. Indels in uninserted alleles were assessed by HTS in PCR amplicons excluding *P2A-EGFP* inserted alleles (see **Extended Data Fig.1g** for method details).
b, The percentages of top on-target indels within uninserted alleles after Cas9-mediated *EGFP-P2A* (798 bp) insertion at the *ACTB* locus. Related to **Fig. 1f**. Indels in uninserted alleles were assessed by HTS in PCR amplicons excluding *EGFP-P2A* inserted alleles (see **Extended Data Fig.1g** for method details).

Supplementary Fig. 3 | Integration of *LIPA* cDNA into the *AAVS1* locus in homozygous *LIPA*$^{894G>A}$ mutant HEK293T cells

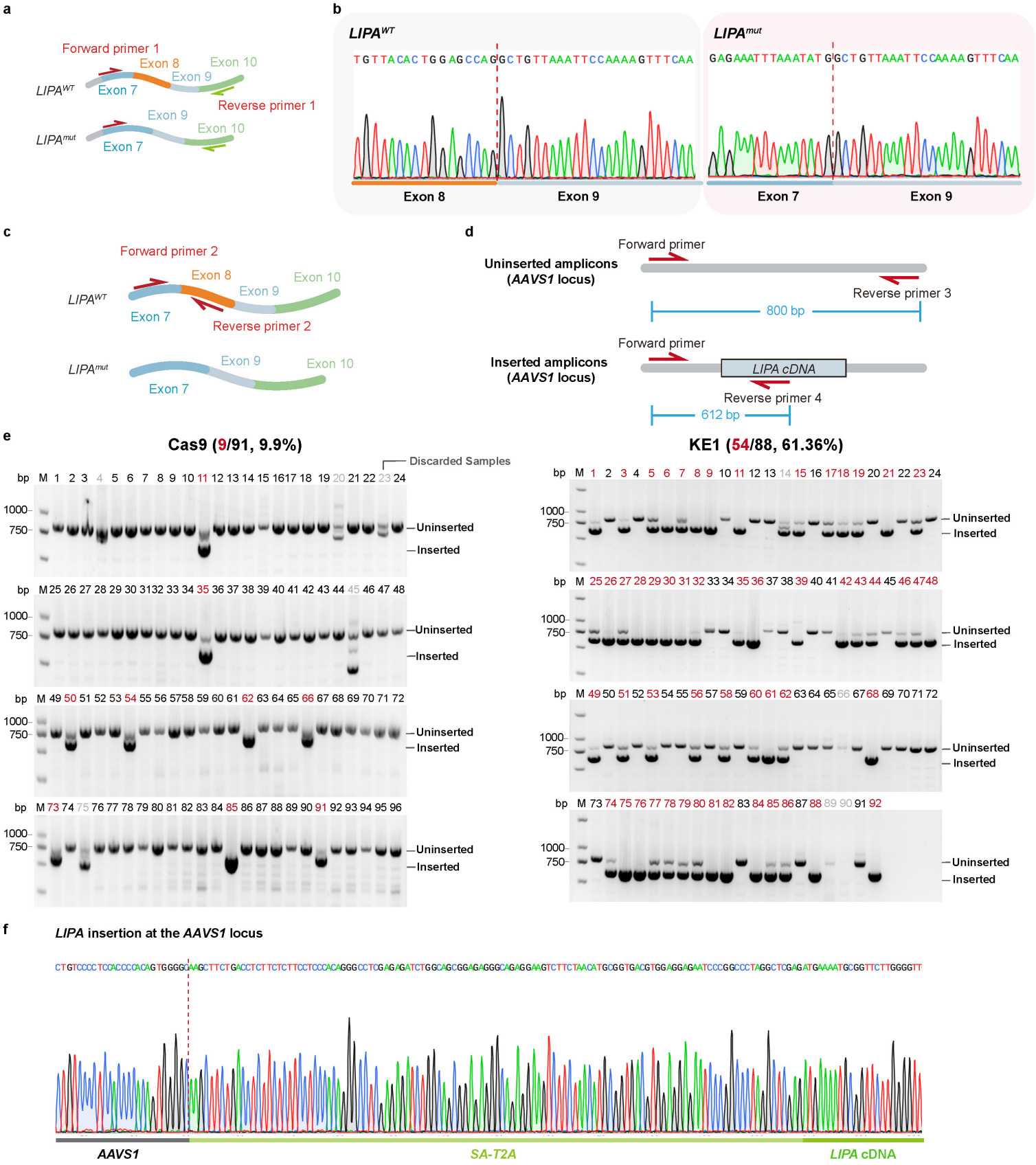

a, Design of RT-PCR primers spanning exons 7 and 10 used in **Fig. 4e** (top).
b, Sanger sequencing of RT-PCR amplicons comparing mRNA sequences in wild-type cells and homozygous *LIPA*$^{894G>A}$ mutant cells.
c, Design of wild-type-specific primers used in **Fig. 4f**, **i** (right) to quantify the expression of wild-type *LIPA*^{WT} mRNA in different groups.
d, Design of three primers for genotyping single-cell clones to identify cells with *LIPA*^{WT} cDNA insertion (1655 bp) into the *AAVS1* locus in the homozygous *LIPA*$^{894G>A}$ mutant cells. The uninserted alleles can be amplified by the Forward primer and Reverse primer 3, generating 800 bp insertion-free amplicons, and the inserted alleles can be amplified by the Forward primer and Reverse primer 4, resulting 612 bp insertion-specific amplicons showing the alleles with successful insertions. These two insertion-free and insertion-specific amplicons can serve as internal controls for each other.
e, Agarose gel analysis of the PCR amplicons for genotyping single-cell clones with *LIPA*^{WT} insertion at the *AAVS1* locus in the homozygous *LIPA*$^{894G>A}$ mutant cells, using the three primers in **d**. Each single-cell clone was assigned a unique identifier. The inserted alleles were amplified using the Forward primer and Reverse primer 4 (as shown in **d**), producing 612 bp insertion-specific amplicon for successful insertions. Uninserted alleles were amplified with the Forward primer and Reverse primer 3 (as shown in **d**), generating 800 bp insertion-free amplicon. The insertion-free and insertion-specific amplicons can serve as internal controls for each other. Any clone lacking both detectable insertion-free and insertion-specific amplicons (may due to lack of amplifiable genomic DNA) were excluded from further analysis, indicated by grey numbering. Additionally, single-cell clones that showed more than two bands (beyond the expected inserted and uninserted amplicons) were excluded. Specifically, the single-cell clones numbered 4, 20, 23, 45 and 75 in the Cas9-treated group, and 14, 66, 89, and 90 in the KE1-treated group, which either lacked undetectable amplicons at both 800 bp (uninserted amplicons) and 612 bp (inserted amplicons) sizes, or exhibited more than two bands, were excluded from further analysis. Related to **Fig. 4g**. See **Supplementary Fig. 4**.
f, Validation of the KE1-mediated insertion of LIPA-expressing cassette at the *AAVS1* locus by Sanger sequencing of insertion-specific PCR amplicons in **e**.

Supplementary Fig. 4 | Uncropped original gel images

a Related to Fig. 4e top

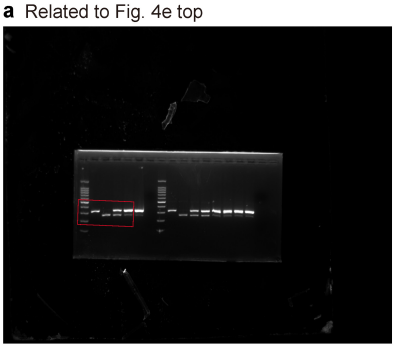

b Related to Fig. 4e bottom

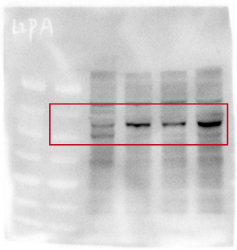

Related to Fig. 4e bottom

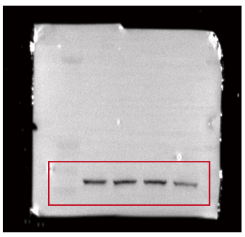

c Related to Extended Data Fig. 8g

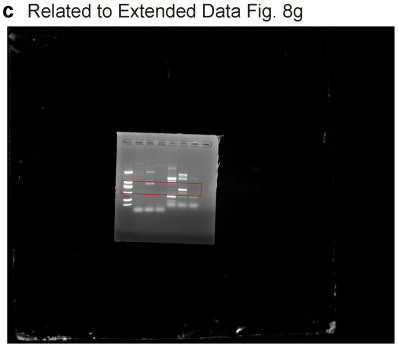

d Related to Extended Data Fig. 9b (left)

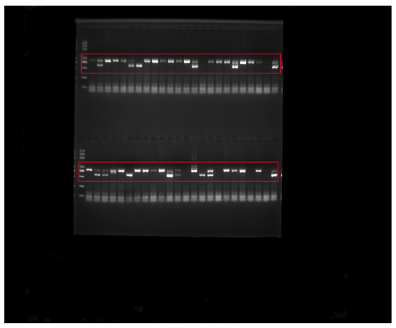

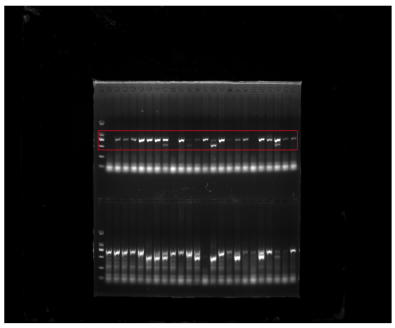

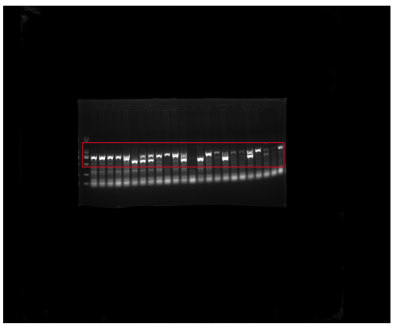

e Related to Extended Data Fig. 9b (right)

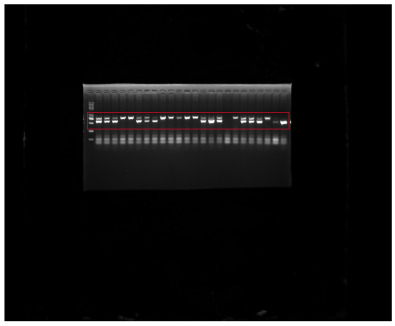

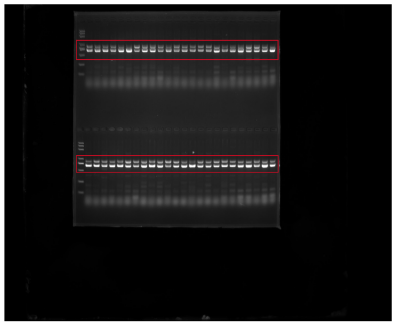

f Related to Extended Data Fig. 9e (left)

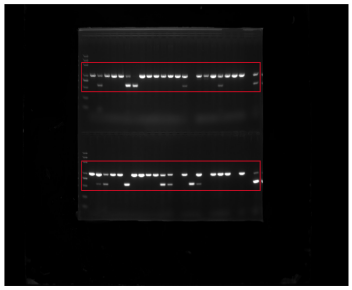

g Related to Extended Data Fig. 9e (right)

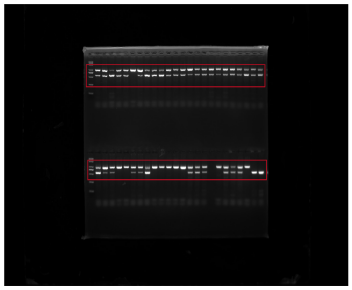

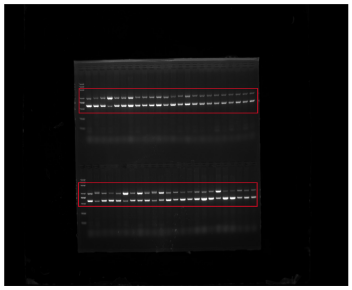

h Related to Supplementary Fig. 3e (left)

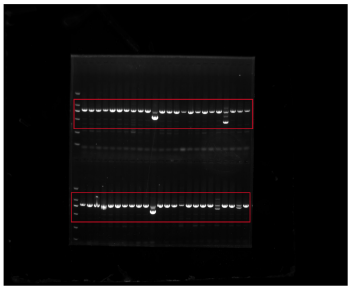

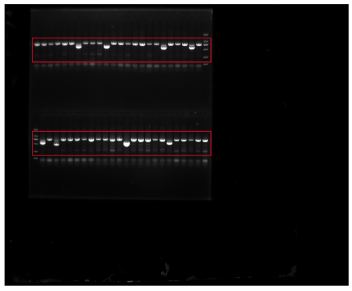

i Related to Supplementary Fig. 3e (right)

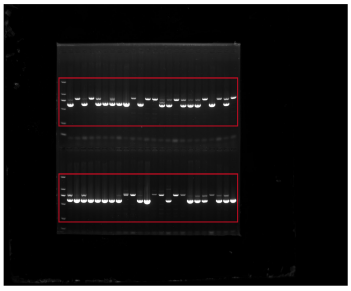

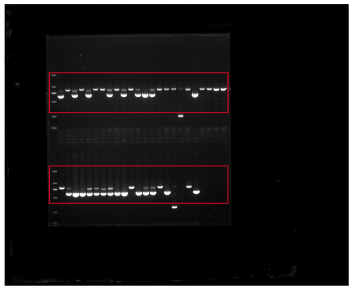

a, Full unedited agarose gel for **Fig. 4e** (top). Red box indicates the region shown in the main figure. **b**, Full unedited gels for **Fig. 4e** (bottom). Red boxes indicate the regions shown in the main figure. Equal volumes of the same samples were analyzed on separate gels/blots processed in parallel. Blots were probed with antibodies against LIPA and GAPDH, respectively. GAPDH served as a sample processing control, and the blotting results were used for qualitative assessment of wild-type protein expression, but not for quantitative analysis. **c**, Full unedited agarose gel for **Extended Data Fig. 8g**. Red box indicates the region shown in the figure. **d**, Full unedited agarose gels for **Extended Data Fig. 9b** (left, Cas9). Red boxes indicate the regions shown in the figure. **e**, Full unedited agarose gels for **Extended Data Fig. 9b** (right, KE1). Red boxes indicate the regions shown in the figure. **f**, Full unedited agarose gels for **Extended Data Fig. 9e** (left, Cas9). Red boxes indicate the regions shown in the figure. **g**, Full unedited agarose gels for **Extended Data Fig. 9e** (right, KE1). Red boxes indicate the regions shown in the figure. **h**, Full unedited agarose gels for **Supplementary Fig. 3e** (left, Cas9). Red boxes indicate the regions shown in the figure. **i**, Full unedited agarose gels for **Supplementary Fig. 3e** (right, KE1). Red boxes indicate the regions shown in the figure.

Supplementary Tables

Supplementary Table 1 sgRNA sequences used in the study[1-4]

Target site	Sequence	Purpose
*ACTB*_sgRNA1	CGCGGCGATATCATCATCCA	Insertion
*ACTB*_sgRNA2	CTCGTCGTCGACAACGGCTC	
RAB11A	GGTAGTCGTACTCGTCGTCG	
H2B	GCGAGCGCCAGGTCCCGGCA	
AAVS1	GGGGCCACTAGGGACAGGAT	
*LIPA*_sgRNA2	TGTCTTATGTTTCCGAGACC	
Rosa26	CAGACCTCCATCGCGCACTC	
HEK4	GGCACTGCGGCTGGAGGTGG	
TRAC	AGAGTCTCTCAGCTGGTACA	
Non-target	GGTCTTCGAGAAGACCT	
*LIPA*_sgRNA1	ATGTTACACTGGAGCCAGGT	Generation of HEK293T cell lines with *LIPA*$^{894G>A}$

Supplementary Table 2 Plasmids used in the study

Plasmid	**Source**	**Identifier**
p*Sp*Cas9-2A-Puro (PX459)[5]	Addgene	48139
pHRdSV40-NLS-dCas9-24xGCN4_v4-NLS-P2A-BFP-dWPRE[6]	Addgene	60910
pHR-scFv-GCN4-sfGFP-GB1-dWPRE[6]	Addgene	60907
p*Sp*Cas9^{D10A}-T2A-Puro	This paper	N/A
p*Sp*Cas9^{D10A}-mSA-T2A-Puro	This paper	N/A
p*Sp*Cas9^{D10A}-SunTag-P2A-ScFv-mSA-T2A-Puro	This paper	N/A
phRAD51*-*Sp*Cas9^{D10A}-mSA-T2A-Puro	This paper	N/A
pCtIP-*Sp*Cas9^{D10A}-mSA-T2A-Puro	This paper	N/A
pDN1S-*Sp*Cas9^{D10A}-mSA-T2A-Puro	This paper	N/A
pET28b-NLS-*Sp*Cas9-NLS-6×His	This paper	N/A
pET28b-NLS-*Sp*Cas9^{D10A}-NLS-mSA-NLS-6×His	This paper	N/A
pHAGE-EF1α-CD19BBz-P2A-mCherry	This paper	N/A
pHAGE-EF1α-CD19-P2A-EGFP	This paper	N/A

Supplementary Table 3 Main reagents used in the study

Reagent	**Source**	**Identifier**
RPMI 1640 medium	Gibco	Cat #11875093
Non-Essential Amino Acids (NEAA)	Gibco	Cat #11140050
GlutaMax	Gibco	Cat #35050061
Sodium Pyruvate	Gibco	Cat #11360070
X-VIVO 15 medium	Lonza	Cat #04-418Q
EasySep™ Human T Cell Isolation Kit	Stem cell technologies	Cat #17951
Dynabeads™ Human T-Activator CD3/CD28 beads	Thermo Fisher Scientific	Cat #11161D
Recombinant Human IL-2	PeproTech	Cat #200-02
Recombinant Human IL-7	PeproTech	Cat #200-07
Recombinant Human IL-15	PeproTech	Cat #200-15
Lipofectamine 3000 reagent	Invitrogen	Cat #L3000015
NU7441	MCE	Cat #HY-11006
AZD-7648	MCE	Cat #HY-111783
M3814	MCE	Cat #HY-101570

NU7026	MCE	Cat #HY-15719
Thymidine	Sigma-Aldrich	Cat #T9250-1G
Nocodazole	MCE	Cat #HY-13520
HiScribe™ T7 mRNA Kit	NEB	Cat #E2080S
HiScribe™ T7 Quick High Yield RNA Synthesis Kit	NEB	Cat #E2050L
Neon™ NxT Electroporation System 10 μL kit	Thermo Fisher Scientific	Cat #N1096
Fixable Viability Stain 510	BD Horizon	Cat #564406
Myc-Tag (9B11) Mouse mAb (Pacific Blue™ Conjugate)	Cell Signaling Technology	Cat #64584
Myc-Tag (9B11) Mouse mAb (Alexa Fluor® 488 Conjugate)	Cell Signaling Technology	Cat #2279
Myc-Tag (9B11) Mouse mAb (Alexa Fluor® 647 Conjugate)	Cell Signaling Technology	Cat #2233

Supplementary Table 4 Sequences of the primers for donor preparation

Name	**Sequence**
*ACTB*_F11	CTGGGACTCAAGGCGCTAACT
*ACTB*_R11	CGATGGGGTACTTCAGGGTGAG
*ACTB*_F12	TTCGCCCGTGCAGAGCCG
*ACTB*_R12	TACAGGGATAGCACAGCCTG
*H2B*_F11	CTAAGCCGCGTTTGTACTGT
*H2B*_R11	AAATGACAGCCGAACTCAGC
*AAVS1*_F11	TGCTTTCTCTGACCTGCATTC
*AAVS1*_R11	AGAGCAGAGCCAGGAACCCCTG
*RAB*_F11	GGTAGCTAGGAGTTCCAGGAC
*RAB*_R11	ACGATGTGGGAGAAGGCAGT
*LIPA*_F1	CAGTTGGTGTTTTCAGCGTT
*LIPA*_R1	AAGGTGCCAGGTTCTGTG
*Rosa*_F1	CTCGGCTAGGTAGGGGATCG
*Rosa*_R1	CCAGCTACAGCCTCGATTTG
*TRAC*_F1	GCCCAGCCTAAGTTGGGGAG
*TRAC*_R1	TGGACTGCCAGAACAAGGCTC
*HEK4*_F1	GTAGGGGAATGTAAACAGGAAAACAG
*HEK4*_R1	TCCCCTCCCCTAGCAGCCCT

Supplementary Table 5 Sequences of the primers used for HTS of on-target indels

Usage	**Name**	**Sequence**
The first round	*ACTB*_Out_F1	CCTTTGGGCGCTAACTGCGT
	*ACTB*_Out_R1	TCGTCCCAGTTGGTGACGAT
	*H2B*_Out_F1	TTCGGAGCCCTAATTTGCAT
	*H2B*_Out_R1	GCTGAATTGTGTCCTGGAGT
	*RAB*_Out_F1	GGCACGGTAGCTCGAGAAATG
	*RAB*_Out_R1	AAGAGAGATGGTGGGAGGAGC
	*TRAC*_Out_F1	TGGTAATGTGATAGATTTCCCAACTTAATGCCAAC ATACCATAAACC
	*TRAC*_Out_R1	CCACCTTCTCTTCATCTGCTTTTTTCCCGTGTC
The second round	Inner primer F2	AATGATACGGCGACCACCGAGATCTACACNNNNN NACACTCTTTCCCTACACGACGCTCTTCCGATCT**NE STEDPRIMER**
	Inner primer R2	CAAGCAGAAGACGGCATACGAGATNNNNNNGTGA CTGGAGTTCAGACGTGTGCTCTTCCGATCT**NESTED PRIMER**
	Nested_*ACTB*_F	AAGGACTCGGCGCGCCGGAAGT
	Nested_*ACTB*_R	CGCCCGCGAAGCCGGCCTT

	Nested_*H2B*_F	GAGCTGGCCAAGCACGCCGT
	Nested_*H2B*_R	CTAGTGATTAGGTGGGTGGCTCTG
	Nested_*RAB*_F	CTCTTCACCCAGTCCGGCAG
	Nested_*RAB*_R	GGCCGGCACGAGGGTCCAC
	Nested_*TRAC*_F	CACTGGCATCTGGACTCCAGCC
	Nested_*TRAC*_R	GGCCACAGCACTGTTGCTCTTG

Supplementary Table 6 PEM-seq adapters and primers

Name	Sequence	Modification
Bridge adapter-upper	CCACGCGTGCTCTACANNNTNNNNTNNNAGATCGGAAGAGCACACGTCTGAACTCCAGT	5'-PO_4, 3'-NH_2
Bridge adapter-lower	TGTAGAGCACGCGTGGNNNNNN	3'-NH_2
*ACTB*_BF1	GCTTCCTTTGTCCCCAATCT	5'-Biotin
*ACTB*_I5_ Nested primer	ACACTCTTTCCCTACACGACGCTCTTCCGATCTAAGGACTCGGCGCGCCGGAAGT	
*RAB11A*_BF1	CTCTTCACCCAGTCCGGCAG	5'-Biotin
*RAB11A*_I5_ Nested primer	ACACTCTTTCCCTACACGACGCTCTTCCGATCTTGGTCCCACAGATACCACTGC	
P7_I7_R1_6 nt index	CAAGCAGAAGACGGCATACGAGATNNNNNNGTGACTGGAGTTCAGACGTGTGC	
P5_I5_F1_6 nt index	AATGATACGGCGACCACCGAGATCTACACNNNNNNACACTCTTTCCCTACACGACGC	
P7_I7_R1_10 nt index	CAAGCAGAAGACGGCATACGAGATNNNNNNNNNNGTGACTGGAGTTCAGACGTGTGC	
P5_I5_F1_10 nt index	AATGATACGGCGACCACCGAGATCTACACNNNNNNNNNNNACACTCTTTCCCTACACGACGC	
EGFP_BF1	CCGCCCTGAGCAAAGACCCCAAC	5'-Biotin
*ACTB*_I5_ Nested_HA	ACACTCTTTCCCTACACGACGCTCTTCCGATCTCGCCCGTGCTCAGGGCTTCTTG	

*ACTB*_BF2	CCTTTGGGCGCTAACTGCGT	5'-Biotin
*ACTB*_OT_I5_ Nested primer	ACACTCTTTCCCTACACGACGCTCTTCCGATCTCCCGT GCTCAGGGCTTCTTG	
*TRAC*_BF1	AATGTGATAGATTTCCCAACTTAATGCCAAC	5'-Biotin
*TRAC*_I5_ Nested primer	ACACTCTTTCCCTACACGACGCTCTTCCGATCTGCAAA GAGGGAAATGAGATCATGTCCTAAC	
CAR-BF1	CCGGCGGCATGGACGAGCTG	5'-Biotin
*TRAC*_OT_I5_ Nested primer	ACACTCTTTCCCTACACGACGCTCTTCCGATCTTTGGT GGTCTCGGCCTTATCCATTG	
*AAVS1*_BF1	ACAGCATGTTTGCTGCCTCC	5'-Biotin
*AAVS1*_I5_ Nested primer	ACACTCTTTCCCTACACGACGCTCTTCCGATCTCTTAT ATTCCCAGGGCCGGT	
P7-Tag	CAAGCAGAAGACGGCATACGAGAT	

Supplementary Table 7 Sequences of the primers used for qPCR, translocations and genotyping

Genetic site	Sequence	Figures
*T2A-IL2RG*_qF1	TCTTCTAACATGCGGTGACGTGG	Fig. 4b
*IL2RG*_qR1	GGTCAGGAAGAAATCAGCTGTGGT	
*LIPA*_mF1	GAAGTGGCTGGGTACCCACG	Fig. 4e
*LIPA*_mR1	CCAGACTGCAGTCGGCACAAG	
*LIPA*_qF1	CCCAGAGTGCGTTTTTGAAGTGG	Fig. 4f,i
*LIPA*_qR1	AGTTCCAGCAGGAGAATGTGTTGT	
*GAPDH*_qF1	CGAGATCCCTCCAAAATCAAGTG	
*GAPDH*_qR1	GGGCAGAGATGATGACCCTTTT	
*ACTB*_F1	CCTTTGGGCGCTAACTGCGT	Extended Data Fig. 8g
*RAB*_R1	GGGGAAAGGAATTCGACGAT	
*RAB*_F2	CCCCGGAAGTACTTCCCCTT	Extended Data Fig. 8g
*ACTB*_R2	TCGTCCCAGTTGGTGACGAT	
*AAVS1*_gF1	GTTTGCTGCCTCCAGGGATC	Extended Data Fig. 9a,b, corresponding to the forward primer and reverse primers 1 and 2.
*AAVS1*_gR1	CTGCTCTGGGCGGAGGAATA	
*AAVS1*_IL2RG	TTCCCGTGGGTCCTGGAGCT	
*AAVS1*_gF2	CTTTGAGCTCTACTGGCTTCTG	Extended Data Fig. 9d,e,

*AAVS1*_gR2	AGAGATGGCTCCAGGAAATG	corresponding to the forward primers 1 and 2 and reverse primer 3.
*AAVS1*_IL2RG2	AACGACTCTGCCTCGTCAG	
*AAVS1*_gF1	GTTTGCTGCCTCCAGGGATC	Supplementary Fig. 3d,e, corresponding to the forward primer and reverse primers 3 and 4.
*AAVS1*_gR1	CTGCTCTGGGCGGAGGAATA	
*AAVS1*_LIPA	CCAGGTATTTCCTCTGCTGTTGC	
*PARP1*_qF	GCCATACGTCTCAGGGAGACC	Extended Data Fig. 2b
*PARP1*_qR	AGCTGAAGGATCAGGGGTAGTT	
*RAD51*_qF	TCTCTGGCAGTGATGTCCTGGA	
*RAD51*_qR	TAAAGGGCGGTGGCACTGTCTA	
*BRCA2*_qF	GGCTTCAAAAAGCACTCCAGATG	
*BRCA2*_qR	GGATTCTGTATCTCTTGACGTTCC	
*IFNB1*_qF	CTTGGATTCCTACAAAGAAGCAGC	Extended Data Fig. 10e
*IFNB1*_qR	TCCTCCTTCTGGAACTGCTGCA	
*NOXA*_qF	CTGGAAGTCGAGTGTGCTACTC	Extended Data Fig. 10f
*NOXA*_qR	TGAAGGAGTCCCCTCATGCAAG	

Supplementary Notes

Supplementary Note 1

Investigating the molecular mechanisms of KNIT editing

Since the DNA donors used in KNIT editing contain homology arms (HAs), we proposed that efficient gene knock-in occurs via HDR at single-nicks. To test this and evaluate the alternative possibilities of NHEJ or MMEJ (microhomology-mediated end joining), we examined whether sequence homology in the HAs of dsDNA donors is required for *EGFP-P2A* insertion at the *ACTB* locus. We designed three modified donor variants: i) replacing the HAs with non-homologous sequences of the same length, ii) removing the entire HAs, and iii) substituting the long HAs with short 25 bp homologous sequences that may support MMEJ (**Extended Data Fig. 2a, top**). The donor variants and the original HA-bearing donor were biotinylated and separately co-transfected into HEK293T cells alongside with nCas9-mSA/sgRNA plasmids. Compared to the original donor with homologous sequences, all modified donors failed to support efficient *EGFP* knock-in (**Extended Data Fig. 2a, bottom**). These results demonstrate that homologous sequences are critical for KNIT editing at single nicks, supporting a single-nick HDR process.

To further investigate the molecular players involved, we examined three DNA repair proteins: RAD51 and BRCA2, two key players of HDR process, as well as PARP1, a sensor of DNA nicks and DSBs that facilitates recruitment of downstream repair

factors[7,8] **(Extended Data Fig. 2b, top left)**. HEK293T cells were transduced with lentiviral vectors expressing gene-specific shRNAs, followed by either Cas9- or KNIT editor 1 (KE1)-mediated genome editing to assess the effects of each gene knockdown on *EGFP-P2A* knock-in efficiency at the *ACTB* locus. To avoid any potential off-target effects, we used two independent shRNAs per gene (**Extended Data Fig. 2b, top right**). KE1-mediated DNA insertion efficiency was significantly reduced by shRNA inhibition of any of the three DNA repair proteins: RAD51, BRCA2, or PARP1 (**Extended Data Fig. 2b, bottom**). These results suggest that KNIT editing depends on single-nick HDR pathway, with RAD51 and BRCA2 playing key roles in facilitating efficient gene knock-in.

DSB-induced HDR process is known to be cell-cycle dependent, with higher HDR efficiency during the S and G2 phases[9,10]. To investigate whether KNIT editing is similarly regulated by the cell cycle, we used two known cell cycle inhibitors to induce cell cycle arrest: thymidine, which blocks DNA replication to enrich cells at the G1/S phase[11], and nocodazole, which disrupts microtubule dynamics to arrest cells at the G2/M transition[12] **(Extended Data Fig. 2c, left)**. Compared to cells treated with DMSO, arresting cells in G1/S phase by thymidine significantly reduced KE1-mediated DNA knock-in efficiency at the *ACTB* locus in HEK293T cells, while arresting cells at G2/M transition enhanced the insertion efficiency (**Extended Data Fig. 2c, right**). These

findings indicate that KNIT editing is also regulated by cell cycle progression, supporting its single-nick HDR mechanism.

In summary, our results provide strong evidence that KNIT editing enables precise gene knock-in via a single-nick HDR pathway: (1) KNIT editing required the homologous sequences in the donor template; (2) knockdown of the HDR factors (RAD51 and BRCA2) significantly reduced insertion efficiency; and (3) its cell cycle dependence, with enhanced efficiency during G2/M phase and reduced efficiency in G1 phase, aligns with the known cell cycle regulation of HDR. Collectively, these findings support that KNIT editing enables precise gene knock-in through a single-nick HDR process.

Supplementary Note 2

Theoretical calculations on Cas9-mediated repeated editing with indel-specific sgRNAs

Previously, indel-specific sgRNAs have been used for second-round Cas9-based editing to improve efficiency[13-15], but their efficiency is limited by the dominant indels from the first editing, which can vary by gene locus and require initial indel profiling. At the *H2B* locus, the top indel accounted for only 18.7% of uninserted alleles after the 1st Cas9 editing, with the remaining indels each contributing less than 6%, suggesting that indel-specific sgRNAs are unlikely to significantly enhance insertion efficiency (**Supplementary Fig. 2a**). For the *ACTB* locus, although the dominant indel accounted for 55.32% of uninserted alleles after the 1st Cas9 editing (**Supplementary Fig. 2b**),

achieving a similar 1.7-fold increase in insertion efficiency as seen with KE1 (**Extended Data Fig. 4c**) would require a second-round Cas9 insertion efficiency of 109.5%, which is impractical. Therefore, based on these theoretical calculations, second-round editing with Cas9 using indel-specific sgRNAs is unlikely to enhance editing efficiency to the level achieved by KNIT editing with the same sgRNAs.

Formula for calculation: $\boldsymbol{E_{2nd} \times P_{major\ indel} \times (1\text{-}E_{1st}) + E_{1st} = 1.7 \times E_{1st}}$

Given E_{1st} = 46.4% (1st insertion efficiency), $P_{major\ indel}$ = 55.32% (Percentage of top indels among uninserted alleles) for the *ACTB* locus, the estimated second-round insertion efficiency (E_{2nd}) needs to reach 109.5% to achieve a 1.7-fold increase in insertion efficiency, as seen with KE1, which is impractical.

Moreover, introducing multiple sgRNAs in DSB-based repeated editing may increase the possibility of off-target editing and genomic instability. In contrast, KNIT editing allows repeated editing with the same sgRNA, enhancing both efficiency and accuracy of gene knock-in.

Supplementary Note 3

Generation and validation of homozygous *LIPA*$^{894G>A}$ HEK293T cell lines

We generated LAL-D-associated mutant cells by introducing the *894G>A* mutation in the

LIPA gene into HEK293T cells. RNP complexes were assembled by mixing 75 pmol of sgRNA with 62 pmol of Cas9 in transfection buffer R. The assembled RNP complexes, along with 60 pmol of single-stranded oligonucleotides (ssODNs), were transfected into 2 × 10^5 suspended HEK293T cells following the standard protocol of the Neon Transfection System 10 μL kit (Thermo Fisher Scientific) at 1150 V/20 ms/2 pulses. Three days after electroporation, single-cell sorting was performed. Homozygous $LIPA^{894G>A}$ HEK293T mutant cell lines were verified through genotyping. By RT-PCR analysis using primers spanning exons 7 and 10 and sanger sequencing, we confirmed the absence of exon 8 within *LIPA* mRNA in the homozygous $LIPA^{894G>A}$ mutant cells (**Fig. 4e and Supplementary Fig. 3a,b**).

Supplementary Note 4

Protein expression and purification

Expression plasmids were transformed into Rosetta E. coli BL21 (DE3) for protein production. Bacterial cells were harvested and lysed using lysis buffer (500 mM NaCl, 20 mM Tris-HCl, pH 7.5, 10% glycerol, 20 mM imidazole, 1 mM TCEP and 1 mM PMSF). The lysate was centrifuged at 15,000× g for 60 minutes at 4 °C. The supernatant was then applied to a Ni-NTA gravity column followed by washing with 60 mM imidazole and elution with 250 mM imidazole. Following this, the purified sample was loaded onto Mono S 5/50 GL column (Cytiva) and eluted with a gradient of elution buffer. Elution fractions were concentrated using a 30 kDa molecular weight cut-off centrifugal filter and

further purified using Superdex 200 Increase 10/300 (Cytiva) with S200 buffer (300 mM NaCl, 20 mM Tris-HCl, pH 7.5, 10% glycerol, 1 mM TCEP). The proteins were analyzed by SDS-PAGE and stocked at -80 °C.

Supplementary Note 5

The sequences of KE1 and KE2

>NLS-nCas9^{D10A}-NLS-linker-mSA-NLS (KE1)

MAPKKKRKVGIHGVPAADKKYSIGLAIGTNSVGWAVITDEYKVPSKKFKVLGNT
DRHSIKKNLIGALLFDSGETAEATRLKRTARRRYTRRKNRICYLQEIFSNEMAKV
DDSFFHRLEESFLVEEDKKHERHPIFGNIVDEVAYHEKYPTIYHLRKKLVDSTDK
ADLRLIYLALAHMIKFRGHFLIEGDLNPDNSDVDKLFIQLVQTYNQLFEENPINAS
GVDAKAILSARLSKSRRLENLIAQLPGEKKNGLFGNLIALSLGLTPNFKSNFDLAE
DAKLQLSKDTYDDDLDNLLAQIGDQYADLFLAAKNLSDAILLSDILRVNTEITKA
PLSASMIKRYDEHHQDLTLLKALVRQQLPEKYKEIFFDQSKNGYAGYIDGGASQ
EEFYKFIKPILEKMDGTEELLVKLNREDLLRKQRTFDNGSIPHQIHLGELHAILRR
QEDFYPFLKDNREKIEKILTFRIPYYVGPLARGNSRFAWMTRKSEETITPWNFEEV
VDKGASAQSFIERMTNFDKNLPNEKVLPKHSLLYEYFTVYNELTKVKYVTEGMR
KPAFLSGEQKKAIVDLLFKTNRKVTVKQLKEDYFKKIECFDSVEISGVEDRFNAS
LGTYHDLLKIIKDKDFLDNEENEDILEDIVLTLTLFEDREMIEERLKTYAHLFDDK
VMKQLKRRRYTGWGRLSRKLINGIRDKQSGKTILDFLKSDGFANRNFMQLIHDD
SLTFKEDIQKAQVSGQGDSLHEHIANLAGSPAIKKGILQTVKVVDELVKVMGRH

KPENIVIEMARENQTTQKGQKNSRERMKRIEEGIKELGSQILKEHPVENTQLQNE

KLYLYYLQNGRDMYVDQELDINRLSDYDVDHIVPQSFLKDDSIDNKVLTRSDKN

RGKSDNVPSEEVVKKMKNYWRQLLNAKLITQRKFDNLTKAERGGLSELDKAGF

IKRQLVETRQITKHVAQILDSRMNTKYDENDKLIREVKVITLKSKLVSDFRKDFQ

FYKVREINNYHHAHDAYLNAVVGTALIKKYPKLESEFVYGDYKVYDVRKMIAK

SEQEIGKATAKYFFYSNIMNFFKTEITLANGEIRKRPLIETNGETGEIVWDKGRDF

ATVRKVLSMPQVNIVKKTEVQTGGFSKESILPKRNSDKLIARKKDWDPKKYGGF

DSPTVAYSVLVVAKVEKGKSKKLKSVKELLGITIMERSSFEKNPIDFLEAKGYKE

VKKDLIIKLPKYSLFELENGRKRMLASAGELQKGNELALPSKYVNFLYLASHYEK

LKGSPEDNEQKQLFVEQHKHYLDEIIEQISEFSKRVILADANLDKVLSAYNKHRD

KPIREQAENIIHLFTLTNLGAPAAFKYFDTTIDRKRYTSTKEVLDATLIHQSITGLY

ETRIDLSQLGGDKRPAATKKAGQAKKKKEFSGGSSGGSSGSETPGTSESATPESS

GGSSGGSAEAGITGTWYNQSGSTFTVTAGADGNLTGQYENRAQGTGCQNSPYT

LTGRYNGTKLEWRVEWNNSTENCHSRTEWRGQYQGGAEARINTQWNLTYEGG

SGPATEQGQDTFTKVKPSAASGSPKKKRKVGGSPAAKRVKLD

>NLS-nCas9^{D10A}-NLS-24xGCN4-P2A-scFv-linker-mSA-NLS (KE2)

The linker between the light and heavy chains of the scFv was modified.

MAPKKKRKVGIHGVPAADKKYSIGLAIGTNSVGWAVITDEYKVPSKKFKVLGNT

DRHSIKKNLIGALLFDSGETAEATRLKRTARRRYTRRKNRICYLQEIFSNEMAKV

DDSFFHRLEESFLVEEDKKHERHPIFGNIVDEVAYHEKYPTIYHLRKKLVDSTDK

ADLRLIYLALAHMIKFRGHFLIEGDLNPDNSDVDKLFIQLVQTYNQLFEENPINAS

GVDAKAILSARLSKSRRLENLIAQLPGEKKNGLFGNLIALSLGLTPNFKSNFDLAE

DAKLQLSKDTYDDDLDNLLAQIGDQYADLFLAAKNLSDAILLSDILRVNTEITKA

PLSASMIKRYDEHHQDLTLLKALVRQQLPEKYKEIFFDQSKNGYAGYIDGGASQ

EEFYKFIKPILEKMDGTEELLVKLNREDLLRKQRTFDNGSIPHQIHLGELHAILRR

QEDFYPFLKDNREKIEKILTFRIPYYVGPLARGNSRFAWMTRKSEETITPWNFEEV

VDKGASAQSFIERMTNFDKNLPNEKVLPKHSLLYEYFTVYNELTKVKYVTEGMR

KPAFLSGEQKKAIVDLLFKTNRKVTVKQLKEDYFKKIECFDSVEISGVEDRFNAS

LGTYHDLLKIIKDKDFLDNEENEDILEDIVLTLTLFEDREMIEERLKTYAHLFDDK

VMKQLKRRRYTGWGRLSRKLINGIRDKQSGKTILDFLKSDGFANRNFMQLIHDD

SLTFKEDIQKAQVSGQGDSLHEHIANLAGSPAIKKGILQTVKVVDELVKVMGRH

KPENIVIEMARENQTTQKGQKNSRERMKRIEEGIKELGSQILKEHPVENTQLQNE

KLYLYYLQNGRDMYVDQELDINRLSDYDVDHIVPQSFLKDDSIDNKVLTRSDKN

RGKSDNVPSEEVVKKMKNYWRQLLNAKLITQRKFDNLTKAERGGLSELDKAGF

IKRQLVETRQITKHVAQILDSRMNTKYDENDKLIREVKVITLKSKLVSDFRKDFQ

FYKVREINNYHHAHDAYLNAVVGTALIKKYPKLESEFVYGDYKVYDVRKMIAK

SEQEIGKATAKYFFYSNIMNFFKTEITLANGEIRKRPLIETNGETGEIVWDKGRDF

ATVRKVLSMPQVNIVKKTEVQTGGFSKESILPKRNSDKLIARKKDWDPKKYGGF

DSPTVAYSVLVVAKVEKGKSKKLKSVKELLGITIMERSSFEKNPIDFLEAKGYKE

VKKDLIIKLPKYSLFELENGRKRMLASAGELQKGNELALPSKYVNFLYLASHYEK

LKGSPEDNEQKQLFVEQHKHYLDEIIEQISEFSKRVILADANLDKVLSAYNKHRD

KPIREQAENIIHLFTLTNLGAPAAFKYFDTTIDRKRYTSTKEVLDATLIHQSITGLY

ETRIDLSQLGGDKRPAATKKAGQAKKKKEFYPYDVPDYASLGSGSPKKKRKVE

DPKKKRKVDGIGSGSNGSSGSNGPGGSGGGGSGGEELLSKNYHLENEVARLKKG

SGSGEELLSKNYHLENEVARLKKGSGSGEELLSKNYHLENEVARLKKGSGSGEE

LLSKNYHLENEVARLKKGSGSGEELLSKNYHLENEVARLKKGSGSGEELLSKNY

HLENEVARLKKGSGSGEELLSKNYHLENEVARLKKGSGSGEELLSKNYHLENEV

ARLKKGSGSGEELLSKNYHLENEVARLKKGSGSGEELLSKNYHLENEVARLKKG

SGSGEELLSKNYHLENEVARLKKGSGSGEELLSKNYHLENEVARLKKGSGSGEE

LLSKNYHLENEVARLKKGSGSGEELLSKNYHLENEVARLKKGSGSGEELLSKNY

HLENEVARLKKGSGSGEELLSKNYHLENEVARLKKGSGSGEELLSKNYHLENEV

ARLKKGSGSGEELLSKNYHLENEVARLKKGSGSGEELLSKNYHLENEVARLKKG

SGSGEELLSKNYHLENEVARLKKGSGSGEELLSKNYHLENEVARLKKGSGSGEE

LLSKNYHLENEVARLKKGSGSGEELLSKDYHLENEVARLKKGSGSGEELLSKNY

HLENEVARLKKGSGSGQRPQPKKKRKVGSGATNFSLLKQAGDVEENPGPMGPDI

VMTQSPSSLSASVGDRVTITCRSSTGAVTTSNYASWVQEKPGKLFKGLIGGTNNR

APGVPSRFSGSLIGDKATLTISSLQPEDFATYFCALWYSNHWVFGQGTKVELKRG

GGGSSGGGSEVKLLESGGGLVQPGGSLKLSCAVSGFSLTDYGVNWVRQAPGRG

LEWIGVIWGDGITDYNSALKDRFIISKDNGKNTVYLQMSKVRSDDTALYYCVTG

LFDYWGQGTLVTVSSSGGSSGGSSGSETPGTSESATPESSGGSSGGSAEAGITGT

WYNQSGSTFTVTAGADGNLTGQYENRAQGTGCQNSPYTLTGRYNGTKLEWRV

EWNNSTENCHSRTEWRGQYQGGAEARINTQWNLTYEGGSGPATEQGQDTFTKV

KPSAASGSPKKKRKVGGSPAAKRVKLD

Supplementary References

1 Jayavaradhan, R. *et al.* CRISPR-Cas9 fusion to dominant-negative 53BP1 enhances HDR and inhibits NHEJ specifically at Cas9 target sites. *Nat Commun* **10**, 2866, doi:10.1038/s41467-019-10735-7 (2019).

2 Chavez, M., Rane, D. A., Chen, X. & Qi, L. S. Stable expression of large transgenes via the knock-in of an integrase-deficient lentivirus. *Nat Biomed Eng* **7**, 661-671, doi:10.1038/s41551-023-01037-x (2023).

3 Xu, H. *et al.* TriTag: an integrative tool to correlate chromatin dynamics and gene expression in living cells. *Nucleic Acids Res* **48**, e127, doi:10.1093/nar/gkaa906 (2020).

4 Roth, T. L. *et al.* Reprogramming human T cell function and specificity with non-viral genome targeting. *Nature* **559**, 405-409, doi:10.1038/s41586-018-0326-5 (2018).

5 Ran, F. A. *et al.* Genome engineering using the CRISPR-Cas9 system. *Nat Protoc* **8**, 2281-2308, doi:10.1038/nprot.2013.143 (2013).

6 Tanenbaum, M. E., Gilbert, L. A., Qi, L. S., Weissman, J. S. & Vale, R. D. A protein-tagging system for signal amplification in gene expression and fluorescence imaging. *Cell* **159**, 635-646, doi:10.1016/j.cell.2014.09.039 (2014).

7 Kanev, P. B., Atemin, A., Stoynov, S. & Aleksandrov, R. PARP1 roles in DNA repair and DNA replication: The basi(c)s of PARP inhibitor efficacy and resistance. *Semin Oncol* **51**, 2-18, doi:10.1053/j.seminoncol.2023.08.001 (2024).

8 Lahiri, S. *et al.* BRCA2 prevents PARPi-mediated PARP1 retention to protect RAD51 filaments. *Nature* **640**, 1103-1111, doi:10.1038/s41586-025-08749-x (2025).

9 Li, G., Yang, X., Luo, X., Wu, Z. & Yang, H. Modulation of cell cycle increases CRISPR-mediated homology-directed DNA repair. *Cell Biosci* **13**, 215, doi:10.1186/s13578-023-01159-4 (2023).

10 Liao, H., Wu, J., VanDusen, N. J., Li, Y. & Zheng, Y. CRISPR-Cas9-mediated homology-directed repair for precise gene editing. *Mol Ther Nucleic Acids* **35**, 102344, doi:10.1016/j.omtn.2024.102344 (2024).

11 Chen, G. & Deng, X. Cell Synchronization by Double Thymidine Block. *Bio Protoc* **8**, doi:10.21769/BioProtoc.2994 (2018).

12 Lin, S., Staahl, B. T., Alla, R. K. & Doudna, J. A. Enhanced homology-directed human genome engineering by controlled timing of CRISPR/Cas9 delivery. *Elife* **3**, e04766, doi:10.7554/eLife.04766 (2014).

13 Bishop, A. L. *et al.* Double-tap gene drive uses iterative genome targeting to help overcome resistance alleles. *Nat Commun* **13**, 2595, doi:10.1038/s41467-022-29868-3 (2022).

14 Bodai, Z., Bishop, A. L., Gantz, V. M. & Komor, A. C. Targeting double-strand break indel byproducts with secondary guide RNAs improves Cas9 HDR-mediated

genome editing efficiencies. *Nat Commun* **13**, 2351, doi:10.1038/s41467-022-29989-9 (2022).

15 Moller, L. *et al.* Recursive Editing improves homology-directed repair through retargeting of undesired outcomes. *Nat Commun* **13**, 4550, doi:10.1038/s41467-022-31944-7 (2022).